



timsTOF Pro/flex – Four reasons to switch to 4D-Proteomics™ on the timsTOF platform

If you are writing a grant and want some concise arguments for replacing older 3D mass spectrometers with the 4D capable on the timsTOF platform, download this brochure.

[Click Here to Download the Brochure](#)



Neuronal Differentiation of LUHMES Cells Induces Substantial Changes of the Proteome

Johanna Tüshaus, Evans Sioma Kataka, Jan Zaucha, Dmitriy Frishman, Stephan A. Müller, and Stefan F. Lichtenthaler*

Neuronal cell lines are important model systems to study mechanisms of neurodegenerative diseases. One example is the Lund Human Mesencephalic (LUHMES) cell line, which can differentiate into dopaminergic-like neurons and is frequently used to study mechanisms of Parkinson's disease and neurotoxicity. Neuronal differentiation of LUHMES cells is commonly verified with selected neuronal markers, but little is known about the proteome-wide protein abundance changes during differentiation. Using mass spectrometry and label-free quantification (LFQ), the proteome of differentiated and undifferentiated LUHMES cells and of primary murine midbrain neurons are compared. Neuronal differentiation induced substantial changes of the LUHMES cell proteome, with proliferation-related proteins being strongly down-regulated and neuronal and dopaminergic proteins, such as L1CAM and α -synuclein (SNCA) being up to 1,000-fold up-regulated. Several of these proteins, including MAPT and SYN1, may be useful as new markers for experimentally validating neuronal differentiation of LUHMES cells. Primary midbrain neurons are slightly more closely related to differentiated than to undifferentiated LUHMES cells, in particular with respect to the abundance of proteins related to neurodegeneration. In summary, the analysis demonstrates that differentiated LUHMES cells are a suitable model for studies on neurodegeneration and provides a resource of the proteome-wide changes during neuronal differentiation. (ProteomeXchange identifier PXD020044).

LUHMES cells originate from a human female 8-week-old mid-brain (mesencephalon). In a non-differentiated, tumor-like state they proliferate rapidly so that larger cell numbers, for example, for drug screening purposes, can be easily obtained. Moreover, they can differentiate into post-mitotic dopaminergic-like neurons,^[2] which is the primary neuron type affected in PD. Thus, differentiation of LUHMES cells is widely used to investigate neurodegenerative diseases, in particular PD,^[3–6] but also to study and prevent neurotoxicity.^[7,8] Neuronal differentiation is generally reflected by substantial changes in gene expression and within the proteome.^[5,7,9–12] Yet, despite systematic RNA expression studies of LUHMES cells,^[5] little is known about how the differentiation process changes the LUHMES cell proteome. In fact, successful neuronal differentiation of LUHMES cells is typically assumed when an increased protein abundance of only a few selected cellular markers, such as β 3-tubulin and tyrosine hydroxylase, are detected, for example, by

immunoblot or immunocytochemistry.^[2] However, it remains unclear how strongly the proteome changes on a systems level and whether differentiation alters the abundance of proteins related to neurodegeneration and PD. Here, we used label-free quantification (LFQ)-based mass spectrometry and compared the proteome of undifferentiated LUHMES (unLUHMES) and differentiated LUHMES (difLUHMES) cells. Our analysis revealed

Alzheimer's and Parkinson's disease (PD) are among the most common neurodegenerative diseases^[1] and remain non-curable to date. Studying the underlying disease mechanisms and risk genes as well as screening and developing drugs requires suitable cell models. One popular cell model is the Lund human mesencephalic (LUHMES) cell line, which combines the advantages of being of human origin and having neuronal properties.

J. Tüshaus, Dr. S. A. Müller, Prof. S. F. Lichtenthaler
German Center for Neurodegenerative Diseases (DZNE)
Feodor-Lynen-Straße 17, München 81377, Germany
E-mail: stefan.lichtenthaler@dzne.de

J. Tüshaus, Dr. S. A. Müller, Prof. S. F. Lichtenthaler
Neuroproteomics, School of Medicine, Klinikum rechts der Isar
Technical University of Munich
Ismaninger Str. 22, Munich 81675, Germany
E. S. Kataka, Dr. J. Zaucha, Prof. D. Frishman
Department of Bioinformatics, Wissenschaftszentrum Weihenstephan
Technical University of Munich
Maximus-von-Imhof Forum 3, Freising 85354, Germany
Prof. S. F. Lichtenthaler
Munich Cluster for Systems Neurology (SyNergy)
Munich, Germany

 The ORCID identification number(s) for the author(s) of this article can be found under <https://doi.org/10.1002/pmic.202000174>

© 2020 The Authors. *Proteomics* published by Wiley-VCH GmbH. This is an open access article under the terms of the Creative Commons Attribution License, which permits use, distribution and reproduction in any medium, provided the original work is properly cited.

DOI: 10.1002/pmic.202000174

that neuronal differentiation induces significant changes within the LUHMES cell proteome, including the alteration of abundance levels of proteins related to neurodegeneration.

In order to compare the proteome of unLUHMES and difLUHMES cells, unLUHMES cells were differentiated for 6 days using tetracycline, GDNF, and cAMP. On the final day of differentiation, difLUHMES cells displayed morphological features characteristic of neurons such as axons and dendrites (Figure 1A), in agreement with previous reports.^[2,3,5] Cell lysates were processed using the filter-aided sample preparation (FASP) protocol and peptides were subjected to LC-MS/MS analysis on a Q-Exactive HF mass spectrometer followed by label-free protein quantification. In total, 4499 and 4931 proteins were identified in at least 4 out of 5 biological replicates of unLUHMES and difLUHMES cells, respectively (Figure 1B); these data contain proteins of all major cellular organelles (Figure 1B). The overlap of consistently quantified proteins was 76% with 4085 proteins, whereas 414 (8%) and 846 proteins (16%) were only quantified in undifferentiated or differentiated cells indicating differentiation-specific protein production (Figure 1C). Importantly, a uniform manifold approximation and projection (UMAP) plot revealed high homogeneity within the five biological replicates of each condition, whereas unLUHMES and difLUHMES were clearly separated (Figure 1D). This demonstrates substantial changes within the LUHMES proteome during differentiation, which is also seen for the individual proteins in a volcano plot representation (Figure 1E) that includes proteins that were quantified in at least four biological replicates in one group. Proteins above the false discovery (FDR) curve and with a fold-change larger than 4 were considered as differentially abundant proteins in further bioinformatics analyses. Among the 4162 proteins with significant abundance changes upon cell differentiation (FDR $p = 0.05$; $s_0 = 0.1$) representing 78% of the quantified LUHMES cell proteome, 981 proteins had a fold-change higher than 4 and were further analyzed in this manuscript (Table S1, Supporting Information). These include 418 proteins with abundances reduced by 4- to 100-fold in difLUHMES and one protein that was down-regulated by more than 100-fold. Among the up-regulated proteins in difLUHMES cells, 549 proteins showed abundance increases between 4- and 100-fold and 13 proteins with a fold-change increase of over 100, compared to unLUHMES cells (Figure 1E). The top 50 differentially abundant proteins are displayed in a heatmap (Figure 2A).

To describe the proteome changes in terms of functional categories, we next performed pathway enrichment analyses using the Kyoto Encyclopedia of Genes and Genomes (KEGG) and the Gene Ontology (GO) resource. Consistent with the differentiation of the dividing unLUHMES cells into postmitotic, neuronal difLUHMES cells, functional categories for cell proliferation were significantly down-regulated (up-regulated in unLUHMES), while functional categories for neurons were up-regulated (Figure 2B). Specifically, the down-regulated categories include the KEGG pathways “DNA replication” and “cell cycle” as well as the GO terms “chromosomal region” and “helicase activity” (Figure 2B). Specific protein examples are the six central members (MCM2-7) of the minichromosome maintenance (MCM) complex responsible for DNA replication,^[13] the DNA

polymerase delta catalytic subunit (POLD1), as well as NCAPH and NCAPD2 important for chromosome condensation, mutations of which have been reported to cause microcephaly^[14] (Figure 1E).

The significantly increased categories in difLUHMES cells comprise KEGG pathways “dopaminergic synapse” and “synaptic vesicle cycle” as well as GO terms “axon” and “neuron development” (Figure 2B). Consistent with the neuronal differentiation, the group of highly up-regulated proteins include key neuronal marker proteins, such as β 3-tubulin (TUBB3), tau (MAPT), microtubule-associated protein 2 (MAP2), the neuronal migration protein doublecortin (DCX), synapsin 1 (SYN1) as well as neurofilament proteins (NEFL, NEFM), microtubule proteins (TUBB2A, TUBB3, TUBB4A), and proteins with neuronal and synaptic functions, for example, NCAM1, L1CAM, CNTN2, neurofascin, septins, and MDGA1 (Table S1, Supporting Information; Figure 2A), but also proteins that are poorly characterized, yet appear to be tightly linked to neuronal functions (e.g., TAGLN3, SOGA3) or even specifically to dopaminergic neuronal functions (GPRIN3). Several of these proteins, including MAPT (tau) and SYN1, were exclusively detected in difLUHMES cells, indicating very low or no expression of these proteins in unLUHMES cells. Many of these proteins may be used as additional markers to affirm successful differentiation of LUHMES cells in the future. Moreover, several of the strongly up-regulated proteins are tightly linked to neurodegenerative processes or enzymes involved in neurodegeneration, such as TAU and the BACE1 protease substrate MDGA1^[15,16] (Table S1, Supporting Information; Figure 2A). Additionally, protein abundances of the PD-risk gene products PARK1 (SNCA) and PARK5 (UCH-L1) were moderately increased in difLUHMES cells. Interestingly, three gamma subunits of guanine nucleotide-binding proteins (GNG2/3/8), which play a key role in transmembrane signal transduction, were among the top 50 changed proteins after LUHMES cell differentiation (Figure 2A) exemplifying one of the major differences in signaling between difLUHMES and unLUHMES. Taken together, our quantitative proteomic comparison provides compelling evidence that difLUHMES cells are superior to unLUHMES cells for studying neuronal processes, such as disease mechanisms or risk genes related to neurodegeneration.

Given the substantial proteome change during neuronal differentiation and the mesencephalic origin of LUHMES cells, we suspected that difLUHMES cells would share more proteins than unLUHMES cells with primary mesencephalic neurons isolated from mouse brain, in particular with regard to proteins related to neurodegeneration and PD. To test this hypothesis, we compared the proteome of cultured primary murine neurons obtained from the mouse midbrain with the proteomes of unLUHMES and difLUHMES cells (Table S2, Supporting Information). Neurons were isolated at embryonic day E16.5 and cultured for 6 days to ensure recovery from the isolation process and allow the formation of a neuronal network. Because the primary murine neurons and the human LUHMES cells are from different species, a direct quantitative comparison of protein abundance based on LFQ intensities is not possible. Instead, we compared the protein abundances on the basis of intensity-based absolute quantification (iBAQ) values, which

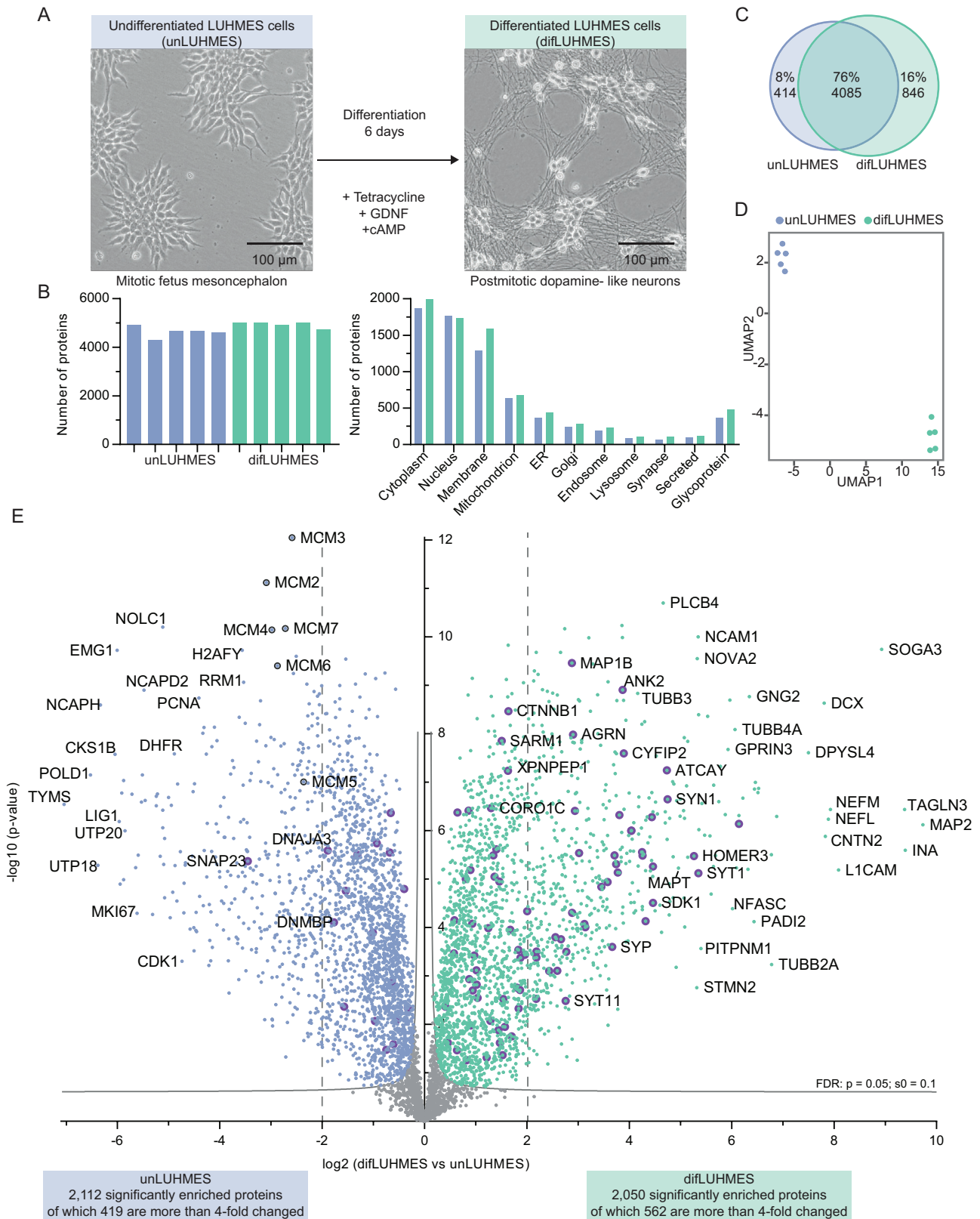


Figure 1. Proteomic characterization of LUHMES cell differentiation. A) Microscopy image of the undifferentiated LUHMES cells (unLUHMES) and the differentiated LUHMES cells (difLUHMES) after 6 days of cultivation in differentiation media containing tetracycline, GDNF, and cAMP. B) Number of proteins quantified in each biological replicate. Proteins detected in at least four out of five biological replicates in one group were considered. C) Venn diagram indicating the overlap between quantified proteins in unLUHMES and difLUHMES cells. D) Uniform Manifold Approximation and Projection

allow estimating protein abundances within a sample,^[17] matching gene names, and protein homologs between murine and human data (Table S2, Supporting Information).

When comparing the iBAQ values of the total quantified proteome, a slightly higher correlation was observed among difLUHMES and unLUHMES cells compared to each of the LUHMES cells against the midbrain neurons (Figure 3A). Likewise, a slightly more substantial overlap of consistently quantified proteins was detected among the LUHMES cells compared to the midbrain neurons (Figure 3B). This was foreseeable since LUHMES cells and midbrain neurons are from different species (i.e., from murine and human). Importantly, however, the pairwise comparison of unLUHMES or difLUHMES with midbrain neurons clearly revealed that the number of shared proteins and in particular of shared PD-related risk proteins was higher between difLUHMES cells and midbrain neurons than for unLUHMES cells (Figure 3B,C). For example, five PD risk proteins (SMPD1, RAB39B, MAPT, TMEM163, STX1B) were consistently not quantified in unLUHMES, but positively detected difLUHMES cells (Figure 3C,E). One of them is the Tau protein (MAPT) with critical roles in neurodegeneration, including PD.^[15] Another PD-related risk protein, which was not quantified in unLUHMES cells, is the sphingomyelin phosphodiesterase SMPD1. Mutations in the SMPD1 gene are associated with an earlier onset of PD and increased α -synuclein levels in cell lines due to SMPD1 knock-out or knock-down.^[18]

Despite the finding that difLUHMES shared more proteins and PD-related proteins with midbrain neurons compared to unLUHMES cells, we also observed that some known neuronal proteins, which are expressed in midbrain neurons, were still not detectably expressed in difLUHMES. One key example is the β -secretase BACE1, a key drug target in Alzheimer's disease.^[19] This protease is neuronally expressed and was indeed detected in the primary midbrain neurons, but was neither detected in unLUHMES nor difLUHMES cells, suggesting that BACE1 protein abundance is much lower in LUHMES cells than in primary neurons. A similar observation was previously made in undifferentiated versus differentiated human neuroblastoma SH-SY5Y cells when compared to primary murine cortical neurons.^[20] While the differentiation process converts the cell lines into neuron-like cells, the example of BACE1 suggests that even after differentiation, the difLUHMES cells still lack some features of primary neurons. Potentially, longer differentiation times or altered differentiation protocols may render the difLUHMES cells even closer to primary neurons.

Taken together, this study provides the first systematic analysis of protein abundance changes during LUHMES cell differentiation. The dramatic proteome changes underline the transformation of a dividing cell line, which allows its easy accessibility, toward a postmitotic neuron useful as an in vitro cell model to study neurodegeneration, such as in PD. Moreover, the proteome of difLUHMES cells shares numerous

neurodegeneration-associated proteins with primary murine midbrain neurons, which emphasizes the value of difLUHMES cells in investigating PD or in the screening for drugs targeting PD-risk genes/proteins. Such approaches often require the generation of targeted gene knock-out cells. This is supported by our study, which provides a resource for unLUHMES and difLUHMES cells that can be mined for the selection of individual proteins to be targeted in knock-out experiments.

Experimental Section

LUHMES Cell Culture: LUHMES cells were cultured and differentiated as described previously.^[2] 0.5 Million undifferentiated LUHMES (unLUHMES) cells were seeded into a Poly-D-Lysine-coated 6-well containing growth media (DMEM F12, 1% N2 Supplement, 0.04 $\mu\text{g mL}^{-1}$ bFGF) and harvested at day 3 in vitro. The live cell count was around 1 million cells using Trypan blue and an automated cell counter (Biorad). For differentiation, 1 million unLUHMES cells were seeded into a Poly-D-Lysine-coated 6-well plate containing differentiation media (DMEM F12, 1% N2 Supplement, 1 $\mu\text{g mL}^{-1}$ tetracycline, 2 ng mL^{-1} GDNF, 500 $\mu\text{g mL}^{-1}$ dibutyl cAMP). At day 6 in vitro, the morphology of the difLUHMES cells was validated under the microscope and the cells were harvested.

Primary Murine Midbrain Neuron Culture: The midbrains were isolated at embryonic day 16.5 from C57BL/6 mice and cultured as described by Kuhn et al.^[24] Briefly, midbrains were isolated; after removal of the meninges, the tissue was digested with papain, dissociated and 1 million living cells were seeded into a Poly-D-Lysine coated 6-well dish using Neurobasal Medium containing B27. The live cell count was determined using Trypan blue and an automated cell counter (Biorad). After 4 h and at day 4 in culture, the medium was exchanged with fresh cultivation media (Neurobasal + B27 + 0.5 mM glutamine + 1% P/S). The neurons were lysed at day 6 in vitro. All animal procedures were performed in accordance with the European Communities Council Directive (86/609/EEC).

Sample Preparation: Cells were washed three times with 1 mL 1x PBS before being lysed in 250 μL of STET buffer (1% Triton X-100, 2 mM EDTA, 150 mM NaCl, 50 mM Tris pH 7.5). The lysate was incubated for 20 min on ice and cleared from cellular debris by a centrifugation step at maximum speed for 10 min at 4 °C. Whole protein concentration was determined with a BCA protein assay kit according to manufacturer's instructions (Interchim, UP40840A). 40 μg of protein extract was digested from each biological replicate using the FASP protocol.^[25] 30 kDa Vivacon filters were used. Desalting was performed using self-made C18 columns for stop-and-go extraction.^[26] Afterward, peptides were dried by vacuum centrifugation and resolved in 0.5% formic acid.

Mass Spectrometry Analysis: Proteome analysis was performed on a LC-MS/MS set up by coupling an EASY-nLC 1200 UHPLC system (Thermo Fischer Scientific) with a Q-Exactive HF Hybrid Quadrupole-Orbitrap mass spectrometer (Thermo Fischer Scientific). 1.5 μg of each biological replicate were injected. A C18 column (30 cm length, 75 μm ID, self-made) packed with ReproSil-Pur 120 C18-AQ resin (Dr. Maisch GmbH, 1.9 μm) was utilized for peptide separation. A binary gradient of mass spectrometry grade H₂O (A) and acetonitrile (B) supplemented with 0.1% v/v formic acid was chosen with a gradient time of 180 min, 50 °C column temperature, and a flow rate of 250 nL min^{-1} : (0 min., 2% B; 3:30 min., 5% B; 137:30 min., 25% B; 168:30 min., 35% B; 182:30 min., 60% B). All samples were analyzed with data-dependent acquisition by choosing the top 15 most abundant peptides for collision-induced dissociation fragmentation. A scan range of 300 to 1400 m/z , full scan at

(UMAP) plot illustrating the separation of the biological replicates of unLUHMES and difLUHMES. E) Volcano plot illustrating the changes in protein levels during LUHMES cell differentiation. Proteins detected in at least four out of five biological replicates in one group are shown after data imputation (down-shifted normal distribution by 1.8 standard deviation and 0.3 width). The negative \log_{10} p -values (y -axis) are plotted against \log_2 -fold-changes of differentiated versus undifferentiated LUHMES cells (x -axis). Permutation-based false discovery-rate (FDR) estimation ($p = 0.05$; $s_0 = 0.1$) is indicated by grey hyperbolic curves and proteins above the FDR curves are considered as significantly regulated. Proteins significantly enriched in unLUHMES and difLUHMES are shown in blue and green, respectively. A purple ring indicates synaptic proteins according to UniProt.

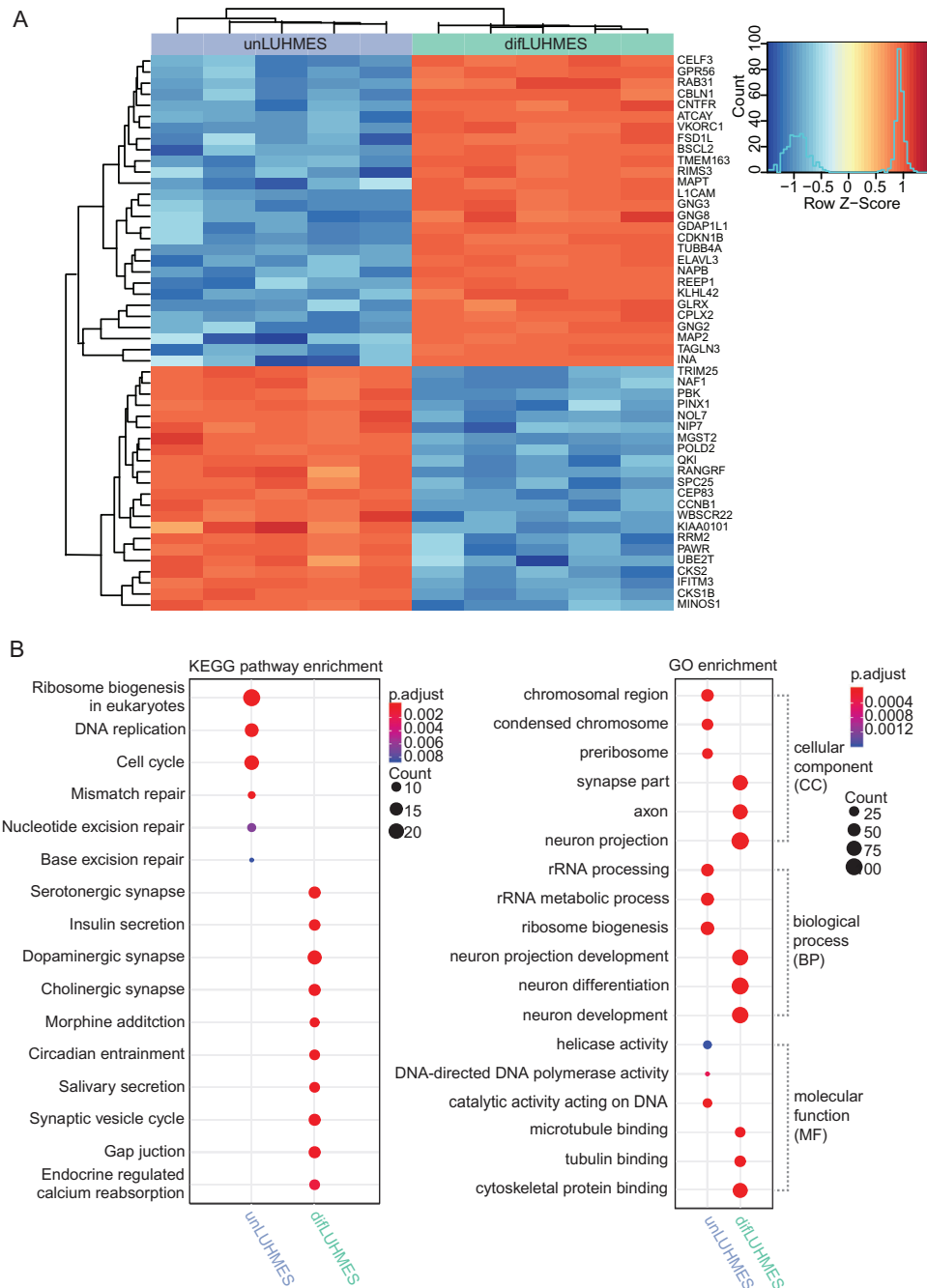


Figure 2. Pathway analysis of LUHMES cells during differentiation. A) The top 50 regulated proteins between unLUHMES and difLUHMES are shown in the heat map (Bonferroni-adjusted p -value < 0.05). Colors follow the z-scored intensity values with red indicating high protein abundance and blue low protein abundance after hierarchical clustering. B) KEGG and GO pathway analysis of the differentially abundant proteins in unLUHMES compared to difLUHMES (Table S2, Supporting Information). Proteins with at least four out of five iBAQ/intensity values in one group were considered. Significantly enriched KEGG pathways and GO terms were determined using Fisher's exact test.^[21] The dot size follows the protein number associated with the enriched GO term/KEGG pathway. The color reflects the significance level (adjusted p -value).

120 000 resolution, maximum injection time (IT) of 50 ms, and automatic gain control (AGC) of 3×10^6 were used for MS1. The following settings were chosen for MS2: Resolution of 15 000; maximum IT of 50 ms; AGC of 1×10^5 ; isolation window of 1.6 m/z ; dynamic exclusion of 120 s.

The raw data were analyzed with MaxQuant (version 1.6.6.0) using default settings with a FDR for protein and peptide of 1%, allowance of two

missed cleavages, fixed carbamidomethylation and N -termini acetylation and methionine oxidation set as variable modifications. However, a minimum peptide length of 6 was chosen. For the human LUHMES samples, the human UniProt reference database (one protein per gene, downloaded on June 12, 2019, with 20 962 entries) was used. For the murine primary neurons, the murine UniProt reference database (one protein per

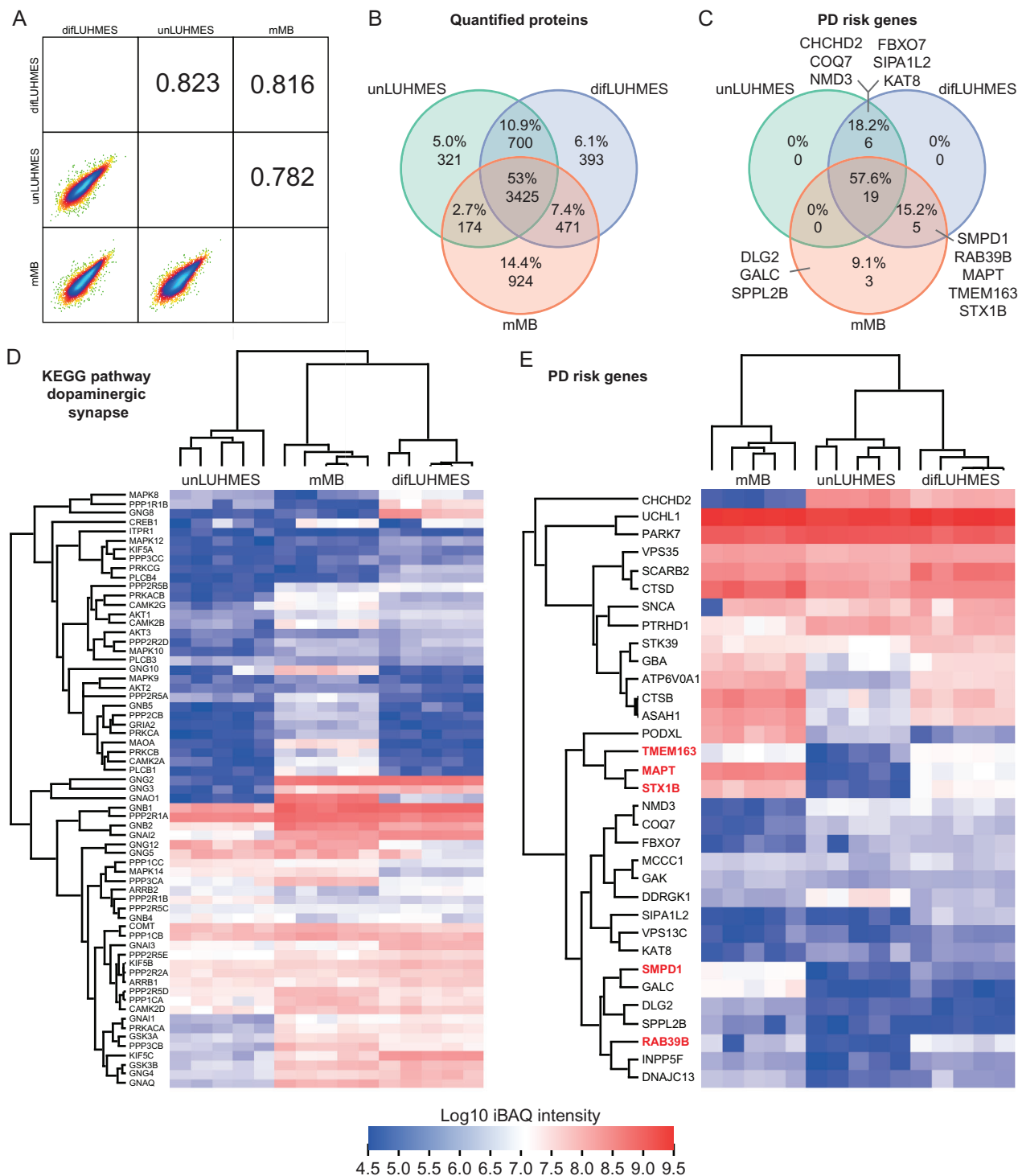


Figure 3. Validation of differentiated LUHMES cells as in vitro disease model. A) Multi-scatter plot of average log₁₀-transformed iBAQ values of unLUHMES, diFLUHMES, and murine midbrain neurons. The density of the protein distribution is illustrated with a color code. B) Venn diagram indicating the overlap between the proteomes of unLUHMES, diFLUHMES, and murine midbrain neurons (left). Matching between human and mouse sequences was performed by gene names and protein orthologs. Proteins were considered in each group if they were quantified in at least four out of five biological replicates on the basis of two unique peptides. C) Venn diagram indicating the overlap between the proteomes of unLUHMES, diFLUHMES, and murine midbrain neurons considering proteins from (B) that were previously annotated as PD-risk genes.^[22,23] D,E) The log₁₀ iBAQ values of proteins from unLUHMES, diFLUHMES, and midbrain neurons visualized in a heat map including proteins of the KEGG pathway dopaminergic synapse (D) or PD-risk genes (E) taken from (C) based on hierarchical clustering (red indicates high, blue indicates low iBAQ values). Proteins highlighted in red were only detected in diFLUHMES and midbrain neurons.

gene, downloaded on June 13, 2019, with 22 290 entries) was used. Data are available via ProteomeXchange with identifier PXD020044.^[27]

Bioinformatics Analysis: Data sets were filtered to retain protein groups consistently quantified. The selected inclusion threshold to consider a protein being quantified in a cell type required LFQ values in four out of the five biological replicates. Unique peptide count and protein group number were determined from the filtered data set. To visualize the relationship between unLUHMES and difLUHMES, dimensionality reduction was performed according to UMAP.^[28] Missing values were imputed by extracting values randomly from a left-shifted Gaussian distribution (shift of 1.8 and scale of 0.3) modeling the lower detection rate.^[29] In the volcano plot, imputed data of all proteins detected in at least four out of five biological replicates in one group (unLUHMES and difLUHMES) were visualized.

Differently Abundant Proteins and Pathway Analysis: The statistical analysis was carried out in the R environment. The data set was filtered to retain proteins with iBAQ/intensity values present for at least four out of the five biological replicates in unLUHMES or difLUHMES. Intensity values were normalized by variance stabilization using the vsn R package.^[30] To enable numerical comparison of protein abundance between unLUHMES and difLUHMES, a one-step imputation was employed. Missing values were replaced, as described above, by extracting values randomly from a left-shifted Gaussian distribution (shift of 1.8 and scale of 0.3) modeling the lower detection rate.^[29] Differentially abundant proteins between unLUHMES and difLUHMES were detected by employing protein-wise linear models combined with the empiric Bayes statistic (implemented in the R package Limma,^[31] similar to ref. [32]). A protein was regarded as differentially abundant if the Bonferroni-corrected *p*-value was below 0.05 and the log₂-fold-change between unLUHMES and difLUHMES was greater than 2.

To understand the biological relevance of the differentially abundant proteins between unLUHMES and difLUHMES, statistically enriched KEGG pathways and Gene Ontology (GO) terms were identified. The enrichment analysis was performed using the R package ClusterProfiler.^[33] To avoid statistical bias,^[34] the background contained only proteins detected in this data set. Fisher's exact test^[21] was applied to calculate the probability of such enrichment by chance. All *p*-values were Bonferroni-adjusted and only terms/pathways with adjusted *p*-values below 0.05 were considered as significantly enriched in unLUHMES or difLUHMES.

Comparison of unLUHMES, difLUHMES, and Primary Midbrain Neurons: To elaborate the overlap between the unLUHMES, difLUHMES, and primary midbrain neuron proteomes, human and murine proteins were matched according to gene names and the JAX homolog database for murine and human genes (URL: <http://www.informatics.jax.org>; Date: 2020-06-24). Only iBAQ quantifications based on at least two unique peptides were considered for further analysis. The iBAQ intensities were normalized between murine midbrain neurons and LUHMES cells using the web-based tool normalizer (<http://normalizer.immunoprot.lth.se/>).^[35] Afterward, data were filtered according to proteins quantified in at least four out of five biological replicates in at least one group. The iBAQ values were log₁₀-transformed and missing values were imputed by extracting values randomly from a left-shifted Gaussian distribution (shift of 1.8 and scale of 0.3) modeling the lower detection rate.^[29] Proteins associated with Parkinson's disease risk were retrieved according to.^[22,23]

Supporting Information

Supporting Information is available from the Wiley Online Library or from the author.

Acknowledgements

S.A.M. and S.F.L. contributed equally to this work. This work was funded by the Deutsche Forschungsgemeinschaft (DFG, German Research Foundation) under Germany's Excellence Strategy within the framework of the Munich Cluster for Systems Neurology (EXC 2145 SyNergy-ID

390857198), the BMBF through CLINSPECT-M and JPND PMG-AD (to S.F.L.). J.T. was supported by a Böhlinger Ingelheim Fonds (BIF) Ph.D. fellowship.

Open access funding enabled and organized by Projekt DEAL.

Conflict of Interest

The authors declare no conflict of interest.

Keywords

dopaminergic neurons, in vitro cell model, LUHMES, neurodegeneration, Parkinson's disease

Received: June 29, 2020

Revised: September 9, 2020

Published online:

- [1] A. Trompetero, A. Gordillo, M. C. Del Pilar, V. M. Cristina, B. Cruz, R. H., *Curr. Pharm. Des.* **2018**, *24*, 22.
- [2] D. Scholz, D. Polt, A. Genewsky, M. Weng, T. Waldmann, S. Schildknecht, M. Leist, *J. Neurochem.* **2011**, *119*, 957.
- [3] X. M. Zhang, M. Yin, M. H. Zhang, *Acta Pharmacol. Sin.* **2014**, *35*, 945.
- [4] M. Hollerhage, C. Moebius, J. Melms, W. H. Chiu, J. N. Goebel, T. Chakroun, T. Koeglsperger, W. H. Oertel, T. W. Rösler, M. Bickle, G. U. Höglinger, *Sci. Rep.* **2017**, *7*, 11469.
- [5] S. E. Pierce, T. Tyson, A. Booms, J. Prah, G. A. Coetzee, *Neurobiol. Dis.* **2018**, *114*, 53.
- [6] D. S. Harischandra, D. Rokad, S. Ghaisas, S. Verma, A. Robertson, H. Jin, V. Anantharam, A. Kanthasamy, A. G. Kanthasamy, *Biochim. Biophys. Acta, Mol. Basis Dis.* **2020**, *1866*, 165533.
- [7] Z. B. Tong, H. Hogberg, D. Kuo, S. Sakamuru, M. Xia, L. Smirnova, T. Hartung, D. Gerhold, *J. Appl. Toxicol.* **2017**, *37*, 167.
- [8] G. Harris, H. Hogberg, T. Hartung, L. Smirnova, *Curr. Protoc. Toxicol.* **2017**, *73*, 11.23.1.
- [9] D. Hornburg, C. Drepper, F. Butter, F. Meissner, M. Sendtner, M. Mann, *Mol. Cell. Proteomics* **2014**, *13*, 3410.
- [10] B. Weiss, S. Haas, G. Lessner, S. Mikkat, M. Kreutzer, M. O. Glocker, A. Wree, O. Schmitt, *Biomed Res. Int.* **2014**, *2014*, 351821.
- [11] C. K. Frese, M. Mikhaylova, R. Stucchi, V. Gautier, Q. Liu, S. Mohammed, A. J. R. Heck, A. F. Maarten Altelaar, C. C. Hoogenraad, *Cell Rep.* **2017**, *18*, 1527.
- [12] J. R. Murillo, L. Goto-Silva, A. Sánchez, F. C. S. Nogueira, G. B. Domont, M. Junqueira, *EuPa Open Proteomics* **2017**, *16*, 1.
- [13] Y. Ishimi, *Genes Genet. Syst.* **2018**, *93*, 125.
- [14] C.-A. Martin, J. E. Murray, P. Carroll, A. Leitch, K. J. Mackenzie, M. Halachev, A. E. Fetit, C. Keith, L. S. Bicknell, A. Fluteau, P. Gautier, E. A. Hall, S. Joss, G. Soares, J. Silva, M. B. Bober, A. Duker, C. A. Wise, A. J. Quigley, S. R. Phadke, Deciphering Developmental Disorders Study; A. J. Wood, P. Vagnarelli, A. P. Jackson, *Genes Dev.* **2016**, *30*, 2158.
- [15] M. Goedert, *Science* **2015**, *349*, 1255555.
- [16] J. Rudan Njavro, J. Klotz, B. Dislich, J. Wanngren, J. R. Njavro, J. Klotz, B. Dislich, J. Wanngren, M. D. Shmueli, J. Herber, P.-H. Kuhn, R. Kumar, T. Koeglsperger, M. Conrad, W. Wurst, R. Feederle, A. Vlachos, S. Michalakis, P. Jedlicka, S. A. Müller, S. F. Lichtenthaler, *FASEB J.* **2020**, *34*, 2465.
- [17] B. Schwanhäusser, D. Busse, N. Li, G. Dittmar, J. Schuchhardt, J. Wolf, W. Chen, M. Selbach, *Nature* **2011**, *473*, 337.
- [18] R. N. Alcalay, V. Mallett, B. Vanderperre, O. Tavassoly, Y. Dauvilliers, R. Y. J. Wu, J. A. Ruskey, C. S. Leblond, A. Ambalavanan, S. B. Laurent,

- D. Spiegelman, A. Dionne-Laporte, C. Liong, O. A. Levy, S. Fahn, C. Waters, S.-H. Kuo, W. K. Chung, B. Ford, K. S. Marder, U. J. Kang, S. Hassin-Baer, L. Greenbaum, J.-F. Trempe, P. Wolf, P. Oliva, X. K. Zhang, L. N. Clark, M. Langlois, P. A. Dion, et al., *Mov. Disord.* **2019**, *34*, 526.
- [19] H. Hampel, R. Vassar, B. De Strooper, J. Hardy, M. Willem, N. Singh, J. Zhou, R. Yan, E. Vanmechelen, A. De Vos, R. Nisticò, M. Corbo, B. Pietrolimbo, J. Streffer, I. Voytyuk, M. Timmers, A. A. T. Monfared, M. Irizarry, B. Albala, A. Koyama, N. Watanabe, T. Kimura, L. Yarenis, S. Lista, L. Kramer, A. Vergallo, *Biol. Psychiatry* **2020**.
- [20] A. Colombo, H. Wang, P.-H. Kuhn, R. Page, E. Kremmer, P. J. Dempsey, H. C. Crawford, S. F. Lichtenthaler, *Neurobiol. Dis.* **2013**, *49*, 137.
- [21] R. A. Fisher, *J. R. Stat. Soc.* **1935**, *98*, 39.
- [22] K. J. Billingsley, S. Bandres-Ciga, S. Saez-Atienzar, A. B. Singleton, *Cell Tissue Res.* **2018**, *373*, 9.
- [23] M. A. Nalls, N. Pankratz, C. M. Lill, C. B. Do, D. G. Hernandez, M. Saad, A. L. DeStefano, E. Kara, J. Bras, M. Sharma, C. Schulte, M. F. Keller, S. Arepalli, C. Letson, C. Edsall, H. Stefansson, X. Liu, H. Pliner, J. H. Lee, R. Cheng, International Parkinson's Disease Genomics Consortium (IPDGC); Parkinson's Study Group (PSG) Parkinson's Research: The Organized GENetics Initiative (PROGENI); Me; GenePD; NeuroGenetics Research Consortium (NGRC); Hussman Institute of Human Genomics (HIHG); Ashkenazi Jewish Dataset Investigator; Cohorts for Health and Aging Research in Genetic Epidemiology (CHARGE); North American Brain Expression Consortium (NABEC); et al., *Nat. Genet.* **2014**, *46*, 989.
- [24] P.-H. Kuhn, K. Koroniak, S. Hogl, A. Colombo, U. Zeitschel, M. Willem, C. Volbracht, U. Schepers, A. Imhof, A. Hoffmeister, C. Haass, S. Roßner, S. Bräse, S. F. Lichtenthaler, *EMBO J.* **2012**, *31*, 3157.
- [25] J. R. Wisniewski, A. Zougman, N. Nagaraj, M. Mann, *Nat. Methods* **2009**, *6*, 359.
- [26] J. Rappsilber, Y. Ishihama, M. Mann, *Anal. Chem.* **2003**, *75*, 663.
- [27] Y. Perez-Riverol, A. Csordas, J. Bai, M. Bernal-Llinares, S. Hewapathirana, D. J. Kundu, A. Inuganti, J. Griss, G. Mayer, M. Eisenacher, E. Pérez, J. Uszkoreit, J. Pfeuffer, T. Sachsenberg, S. Yilmaz, S. Tiwary, J. Cox, E. Audain, M. Walzer, A. F. Jarnuczak, T. Ternent, A. Brazma, J. A. Vizcaíno, *Nucleic Acids Res.* **2019**, *47*, D442.
- [28] M. W. Dorrity, L. M. Saunders, C. Queitsch, S. Fields, C. Trapnell, *Nat. Commun.* **2020**, *11*, 1537.
- [29] X. Zhang, A. H. Smits, G. B. A. van Tilburg, H. Ovaa, W. Huber, M. Vermeulen, *Nat. Protoc.* **2018**, *13*, 530.
- [30] W. Huber, A. von Heydebreck, H. Sultmann, A. Poustka, M. Vingron, *Bioinformatics* **2002**, *18*, S96.
- [31] M. E. Ritchie, B. Phipson, D. Wu, Y. Hu, C. W. Law, W. Shi, G. K. Smyth, *Nucleic Acids Res.* **2015**, *43*, e47.
- [32] K. Kammers, R. N. Cole, C. Tiengwe, I. Ruczinski, *EuPA Open Proteomics* **2015**, *7*, 11.
- [33] G. Yu, L. G. Wang, Y. Han, Q. Y. He, *OMICS: J. Integr. Biol.* **2012**, *16*, 284.
- [34] J. A. Timmons, K. J. Szkop, I. J. Gallagher, *Genome Biol.* **2015**, *16*, 186.
- [35] A. Chawade, E. Alexandersson, F. Levander, *J. Proteome Res.* **2014**, *13*, 3114.